H_2O_2 is that proton transfer may not occur to $\{Fl_T \cdot O_2^{-}\}$. The initial radical pair may diffuse apart or collapse to give 4a-hydroperoxyflavin.

Favaudon[2] has provided the pH dependence for the initial rates of reaction of 1,5-dihydro-FMN with O_2. These are plotted in the form of log $k_{initial}/O_2$ vs. pH in Figure 12A. In Figure 12B there is plotted, as a function of pH, values of $\Delta G^{\ddagger}$ (from the points of Figure 12A) and $\Delta G°$ for the formation of FMN radical and superoxide. The values of $\Delta G^{\ddagger}$ and ΔG^0 have a constant separation of ~30 kJ M^{-1} between pH 2 and pH 7. In the pH profile of Figure 12A, the line has been generated from eq 44 by employing the rate constants $k_1 = 52\ M^{-1}\ s^{-1}$, $k_2 = 404\ s^{-1}$, and $k_3 = 0.54\ s^{-1}$ (at $[O_2] = 1.5 \times 10^{-3}$ M) and the acid dissociation constants $pK_{a_1} = 9.17$, $pK_{a_2} = 4.34$, and $pK_{a_3} = 4.94$. The values of the kinetically apparent acidity terms pK_{a_2} and pK_{a_3} do not correspond to pK_a values of 1,5-dihydro-FMN, FMN radical, or FMN nor to the (anticipated) pK_a of any intermediate hydroperoxide. The pK_{a_3} value does not approximaae that of $HO_2\cdot$. As recognized by Favaudon, the bimolecular rate constant for the reaction of 1,5-dihydro-FMN with O_2 cannot be separated from the ensuing autocatalytic reaction by the use of initial rate constants. It is likely that one or all the acid dissociation constants of eq 49 are

$$\frac{k_{initial}}{[O_2]} = k_1 a_H + \frac{k_2 K_{a_1} a_H}{K_{a_1}K_{a_2} + K_{a_1} a_H + a_H^2} + \frac{k_3 K_{a_3}}{K_{a_3} + a_H} \quad (49)$$

$$A \qquad B \qquad C$$

only apparent acid dissociation constants and are composed of kinetic constants related to the autocatalytic reaction.

Acknowledgment. This work was supported by grants from the National Science Foundation and from the National Institutes of Health.

Registry No. $\mathbf{1}_{red}$, 25431-13-4; $\mathbf{2}_{red}$, 80720-87-2; $\mathbf{3}_{red}$, 50387-36-5; $\mathbf{4}_{red}$, 86969-35-9; $\mathbf{5}_{red}$, 79075-88-0; 3-methyllumiflavin, 18636-32-3; 3-(carboxymethyl)lumiflavin, 20227-26-3; tetraacetylriboflavin, 752-13-6.

Cross Polarization and Magic Angle Sample Spinning NMR Spectra of Model Organic Compounds. 3. Effect of the ^{13}C–^{1}H Dipolar Interaction on Cross Polarization and Carbon–Proton Dephasing

Lawrence B. Alemany, David M. Grant,* Terry D. Alger, and Ronald J. Pugmire

Contribution from the Department of Chemistry, University of Utah, Salt Lake City, Utah 84112. *Received May 13, 1982*

Abstract: Carbon-13 NMR studies involving conventional cross polarization and dipolar dephasing techniques at a variety of contact and delay times, respectively, provide valuable information on the magnitude of ^{13}C–^{1}H dipole–dipole interactions. In solids whose spectra have overlapping resonances, such techniques discriminate between protonated and nonprotonated carbons. In dipolar dephased spectra, dipolar and rotational modulation of the resonances can occur for methine and methylene carbons, which are strongly coupled to the directly bonded protons. Methyl carbons exhibit a very wide range of effective dipolar couplings because of rapid methyl rotation that varies depending upon the structural environment. Dipolar modulation in methyl groups is not observed. Carbon atoms in *tert*-butyl methyl groups experience even weaker effective dipolar interactions than other methyl carbon atoms. These motionally decreased dipolar interactions are similar to those experienced by the quaternary aliphatic carbon atom. Steric crowding of a *tert*-butyl group on an aromatic ring causes (on the average) one of its methyl groups to differ in mobility from the other two. A biexponential decay not evident in any of the other functional groups studied results for both the quaternary and methyl carbons in the *tert*-butyl group. Nonprotonated sp^2-hybridized carbon atoms also exhibit weak dipolar couplings because of the remoteness of protons. The magnitude of the coupling varies substantially as a result of variations in motional freedom and structure.

Introduction

Previous work has shown CP/MAS NMR to be very useful for characterizing and quantitatively studying diamagnetic organic solids.[1,2] The relative polarization rates of different types of protonated carbon atoms were shown to be a direct manifestation of the effective magnitude of the ^{13}C–^{1}H dipolar interaction. Methyl carbons are especially interesting because they exhibit a wide range of effective dipolar couplings resulting from differing degrees of motional freedom. Conventional cross polarization of a carbon is characterized by the time a carbon nucleus receives polarization from the coupled protons.

Alla and Lippmaa[3] were the first to use dipolar dephasing to distinguish between carbon atoms with different effective dipolar couplings. Since then, the method has been applied to single crystals,[4–6] calcium formate and frozen benzene,[7] simple powdered organic compounds,[8–18] biochemical materials,[9,13,19–23] a clathrate,[24] organometallic complexes,[25,26] polymers,[27–34] and fossil fuel sam-

(1) Part 1: Alemany, L. B.; Grant, D. M.; Pugmire, R. J.; Alger, T. D.; Zilm, K. W. *J. Am. Chem. Soc.* **1983**, *105*, 2133–2141.
(2) Part 2: Alemany, L. B.; Grant, D. M.; Pugmire, R. J.; Alger, T. D.; Zilm, K. W. *J. Am. Chem. Soc.* **1983**, *105*, 2142–2147.
(3) Alla, M.; Lippmaa, E. *Chem. Phys. Lett.* **1976**, *37*, 260–264.
(4) Hester, R. K.; Ackerman, J. L.; Neff, B. L.; Waugh, J. S. *Phys. Rev. Lett.* **1976**, *36*, 1081–1083.
(5) Rybaczewski, E. F.; Neff, B. L.; Waugh, J. S.; Sherfinski, J. S. *J. Chem. Phys.* **1977**, *67*, 1231–1236.
(6) Bodenhausen, G.; Stark, R. E.; Ruben, D. J.; Griffin, R. G. *Chem. Phys. Lett.* **1979**, *67*, 424–427.
(7) Stoll, M. E.; Vega, A. J.; Vaughn, R. W. *J. Chem. Phys.* **1976**, *65*, 4093–4098.
(8) Opella, S. J.; Frey, M. H. *J. Am. Chem. Soc.* **1979**, *101*, 5854–5856.
(9) Opella, S. J.; Frey, M. H.; Cross, T. A. *J. Am. Chem. Soc.* **1979**, *101*, 5856–5857.
(10) Gray, G. A.; Hill, H. D. W. *Ind. Res. Dev.* **1980**, *22* (3), 136–140.
(11) Munowitz, M. G.; Griffin, R. G.; Bodenhausen, G.; Huang, T. H. *J. Am. Chem. Soc.* **1981**, *103*, 2529–2533.

0002-7863/83/1505-6697$01.50/0

ples.[17,35-47] Many modifications of the technique have also appeared.[4,6,7,11,12,21,45,47] Dipolar dephasing studies measure the time for a polarized carbon nucleus to lose its magnetization after the proton locking field is terminated. Dipolar dephasing results depend upon the magnitude of the dipolar coupling and generally may be grouped into three cases: CH and CH_2 (strong coupling), CH_3 (moderate coupling), and nonprotonated C (weak coupling).

In the first paper[1] in this series, dipolar dephasing results and relative rates of cross polarization combined to give an unambiguous assignment of resonances. This paper further demonstrates that conventional cross polarization and dipolar dephasing results are complementary[42] and together provide information on the magnitude of dipolar couplings between protons and carbon atoms.

Opella et al.[8,9] and others[1,10,13,14,19,20,22-35,38-41,44,46] have demonstrated that dephasing periods can be selected to yield a spectrum containing only signals of the methyl and nonprotonated carbon atoms. However, a great variety of dephasing times have been used: 40,[13,14,22,27,29,30,34,46] 42,[24] 50,[19,23,31,40,41] 60,[30,38], 75,[35] 80,[39] 100,[1,25,28,33] and 120 μs.[26] Opella's work[8,9] indicated for a dephasing time of 40 μs that the methine and methylene carbon resonances are greatly attenuated if not completely eliminated. Thus, if the goal merely is to obtain a spectrum containing somewhat attenuated signals of only the methyl and nonprotonated carbon atoms, then dephasing periods of 40 to 120 μs suffice. However, a better goal might be to use the shortest dephasing time consistent with eliminating the methine and methylene carbon analysis of complex solids such as polymers and fossil fuels, such optimization is essential.

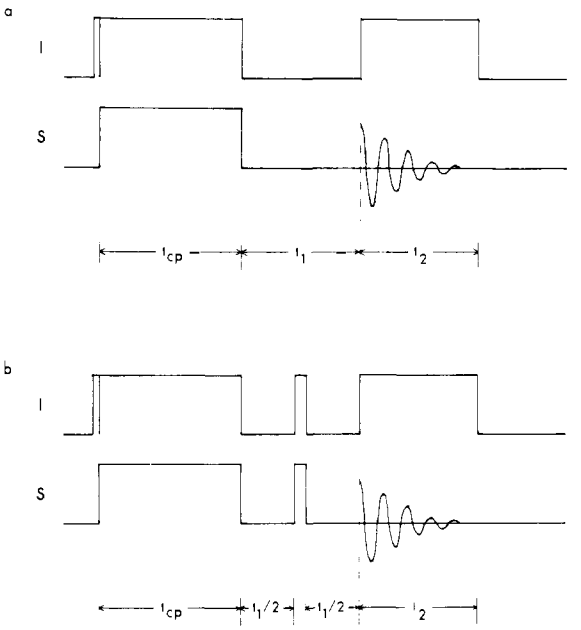

Figure 1. Possible pulse sequences for a dipolar dephasing experiment. In either (a) or (b), a 90° *I*-spin pulse is followed by a 90° phase shift in the *I*-spin rf field so as to create the spin lock before the *S*-spin rf field whose magnitude satisfies the Hartmann–Hahn condition[49] is applied for a time t_{cp}. In (a) both rf fields are then turned off for a time t_1 (the evolution period) before S-spin data acquisition with heteronuclear decoupling occurs for a time t_2 (the detection period). In (b), both rf fields are turned off for a time $t_1/2$; then a 180° pulse (with the same phase as during t_{cp}) is applied to each spin system; both rf fields are again turned off for a time $t_1/2$; and finally, *S*-spin data acquisition with heteronuclear decoupling occurs for a time t_2.

Instead of using just a single dephasing period, some investigators[3,11,12,16,17,36,37,42,43,45,47] have used many values to study a powdered solid in more detail. The reports demonstrate the utility of multiple dephasing times (e.g., norbornadiene,[3] glycine,[11,12] calcium formate,[11,12] sodium acetate,[16] sodium propanoate[16], $MgHPO_3(H_2O)_6$,[16] 3-methylpentanedioic acid,[17] *p*-di-*tert*-butylbenzene,[17] and fossil fuel samples[36,37,42,43,45,47]).

The rapidly increasing number of applications of the dipolar dephasing technique to complex solids has created a need for more quantitative information on the magnitude of such effective dipolar couplings for different carbon atoms.

The dipolar dephasing pulse sequence of Alla and Lippmaa,[3] shown in Figure 1a,[48] measures $T_2(^{13}C)$. Without the two locking rf fields, the *I*–*S* dipolar Hamiltonian evolves for a time t_1, during which the short-term spin order is rapidly dephased both by chemical shift anisotropy and heteronuclear dipolar interactions. Reestablishing the *I* decoupling field at the end of t_1, however, permits the chemical shift Hamiltonian to evolve for a time t_2 while maintainting the dipolar dephasing at the level to which it had evolved during t_1.

(12) Griffin, R. G.; Bodenhausen, G.; Haberkorn, R. A.; Huang, T. H.; Munowitz, M.; Osredkar, R.; Ruben, D. J.; Stark, R. E.; van Willigen, H. *Philos. Trans. R. Soc. Lond., Ser. A* **1981**, *299*, 547–563.
(13) Balimann, G. E.; Groombridge, C. J.; Harris, R. K.; Packer, K. J.; Say, B. J.; Tanner, S. F. *Philos. Trans. R. Soc. Lond., Ser. A* **1981**, *299*, 643–663.
(14) Chippendale, A. M.; Mathias, A.; Harris, R. K.; Packer, K. J.; Say, B. J. *J. Chem. Soc., Perkin Trans. 2* **1981**, 1031–1035.
(15) Munowitz, M.; Bachovchin, W. W.; Herzfeld, J.; Dobson, C. M.; Griffin, R. G. *J. Am. Chem. Soc.* **1982**, *104*, 1192–1196.
(16) Munowitz, M. G.; Griffin, R. G. *J. Chem. Phys.* **1982**, *76*, 2848–2858.
(17) Murphy, P. D.; Cassady, T. J.; Gerstein, B. C. *Fuel* **1982**, *61*, 1233–1240.
(18) Imashiro, F.; Takegoshi, K.; Okazawa, S.; Furukawa, J.; Terao, T.; Saika, A. *J. Chem. Phys.* **1983**, *78*, 1104–1111.
(19) O'Donnell, D. J.; Ackerman, J. J. H.; Maciel, G. E. *J. Agric. Food Chem.* **1981**, *29*, 514–518.
(20) Cross, T. A.; DiVerdi, J. A.; Opella, S. J. *J. Am. Chem. Soc.* **1982**, *104*, 1759–1761.
(21) DiVerdi, J. A.; Opella, S. J. *J.* Am. *Chem. Soc.* **1982**, *104*, 1761–1762.
(22) Woolfenden, W. R.; Grant, D. M.; Straight, R. C.; Englert, E., Jr. *Biochem. Biophys. Res. Commun.* **1982**, *107*, 684–694.
(23) Chang, C.-J.; Diaz, L. E.; Woolfenden, W. R.; Grant, D. M. *J. Org. Chem.* **1982**, *47*, 5318–5321.
(24) Ripmeester, J. A.; Tse, J. S.; Davidson, D. W. *Chem. Phys. Lett.* **1982**, *86*, 428–433.
(25) Damude, L. C.; Dean, P. A. W.; Sefcik, M. D.; Schaefer, J. *J. Organomet. Chem.* **1982**, *226*, 105–114.
(26) Zumbulyadis, N.; Gysling, H. J. *J. Am. Chem. Soc.* **1982**, *104*, 3246–3247.
(27) Fyfe, C. A.; Rudin, A.; Tchir, W. *Macromolecules* **1980**, *13*, 1320–1322.
(28) Schaefer, J.; Sefcik, M. D.; Stejskal, E. O.; McKay, R. A. *Macromolecules* **1981**, *14*, 188–192.
(29) Dilks, A.; Kaplan, S.; Van Laeken, A. *J. Polym. Sci., Polym. Chem. Ed.* **1981**, *19*, 2987–2996.
(30) Kaplan, S.; Dilks, A. *Thin Solid Films* **1981**, *84*, 419–424.
(31) Schröter, B.; Hörhold, H.-H.; Raabe, D. *Makromol. Chem., Macromol. Chem. Phys.* **1981**, *182*, 3185–3193.
(32) Harris, R. K.; Packer, K. J.; Say, B. J. *Makromol. Chem., Suppl. 4* **1981**, 117–127.
(33) Maciel, G. E.; Chuang, I.-S.; Myers, G. E. *Macromolecules* **1982**, *15*, 1218–1220.
(34) Brown, C. E.; Khoury, I.; Bezoari, M. D.; Kovacic, P. *J. Polym. Sci., Polym. Chem. Ed.* **1982**, *20*, 1697–1707.
(35) Miknis, F. P.; Sullivan, M.; Bartuska, V. J.; Maciel, G. E. *Org. Geochem.* **1981**, *3*, 19–28.
(36) Weinberg, V. L.; Yen, T. F.; Gerstein, B. C.; Murphy, P. D. *Prepr., Div. Pet. Chem., Am. Chem. Soc.* **1981**, *26*, 816–824.
(37) Murphy, P. D.; Gerstein, B. C.; Weinberg, V. L.; Yen, T. F. *Anal. Chem.* **1982**, *54*, 522–525.
(38) Gerstein, B. C.; Murphy, P. D.; and Ryan, L. M. In "Coal Structure"; Meyers, R. A., Ed.; Academic Press: New York, 1982; pp 87–129.
(39) Hagaman, E. W.; Woody, M. C. *Proc. Int. Conf. Coal Sci., Dusseldorf, W. Germany, Sept 7–9* **1981**, 807–811.
(40) Kuehn, D. W.; Davis, A.; Snyder, R. W.; Starsinic, M.; Painter, P. C.; Havens, J.; Koenig, J. L. *Am. Chem. Soc., Div. Fuel Chem., Prepr.* **1982**, *27* (2), 55–63.
(41) Havens, J. R.; Koenig, J. L.; Painter, P. C. *Fuel* **1982**, *61*, 393–396.
(42) Sullivan, M. J.; Maciel, G. E. *Anal. Chem.* **1982**, *54*, 1606–1615.
(43) Palmer, A. R.; Maciel, G. E. *Anal. Chem.* **1982**, *54*, 2194–2198.
(44) Dudley, R. L.; Fyfe, C. A. *Fuel* **1982**, *61*, 651–657.
(45) Wilson, M. A.; Collin, P. J.; Pugmire, R. J.; Grant, D. M. *Fuel* **1982**, *61*, 959–967.
(46) Pugmire, R. J.; Woolfenden, W. R.; Mayne, C. L.; Karas, J.; Grant, D. M. *Am. Chem. Soc., Div. Fuel Chem., Prepr.* **1983**, *28* (1), 103–117.
(47) Unpublished work, this laboratory.
(48) The figure in the original paper[3] is incorrect. This is also evident from the discussion in section 3.1 of the original paper.[3]
(49) Hartmann, S. R.; Hahn, E. L. *Phys. Rev.* **1962**, *128*, 2042–2053.

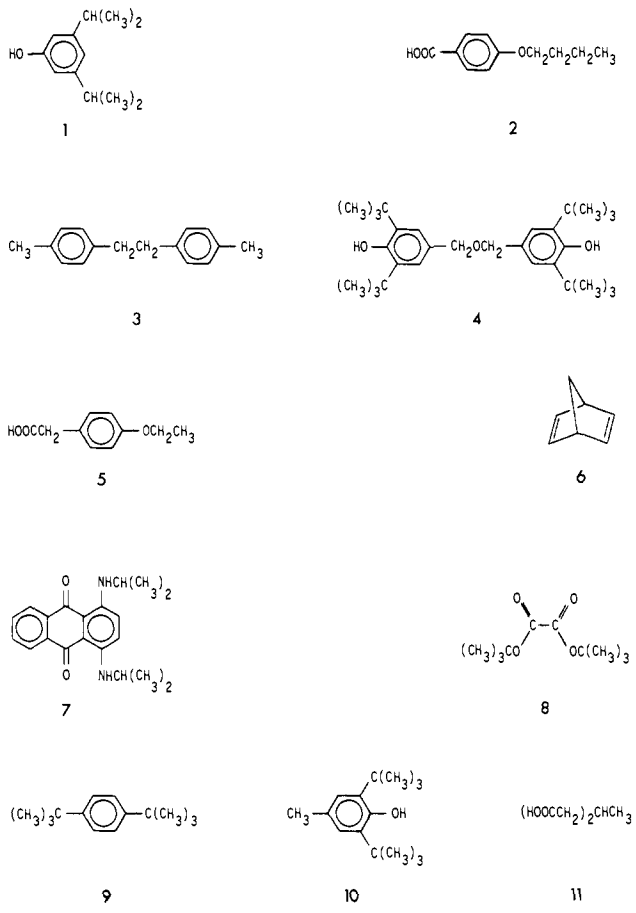

Figure 2. Significant compounds discussed in this paper.

Table I. Approximate Time Required (μs) for Carbon Atom Signal Intensity in Various Functional Groups To Decay by 50 and 75%[a]

functional group	50% decay	75% decay
CH_2	15–30	20–45
	(15–20)	(20–30)
CH	20–40	25–55
	(20–30)	(25–40)
non-*tert*-butyl CH_3	40–90	80–310
	(40–75)	(80–310)
tert-butyl CH_3	410	1300
nonprotonated sp^3	580	1500
nonprotonated sp^2	50–175	165–660
	(50–165)	(165–660)

[a] Values in parentheses do not include data for **5**, many of whose signals decay relatively slowly.

Stoll, Vega, and Vaughn[7] were the first to apply a 180° pulse to the *S* spin to refocus the effects of chemical shifts and other static field inhomogeneities. Bodenhausen et al.[6] first applied a 180° pulse to each nucleus in the middle of the evolution period t_1 (Figure 1b) to remove the effect of an offset (e.g., chemical shift[11,12,15] or quadrupolar splitting[6,12]) on the F_1 dimension of the spectrum while preserving the scalar or dipolar evolution throughout t_1.[11,12] Thus, either pulse sequence shown in Figure 1 yields spectra for liquids[50–52] or solids[6,11,12,15,16] whose signal amplitudes and phases are modulated by the scalar or dipolar Hamiltonian.[6,12,16] However, the simultaneous application of 180° pulses (Figure 1b) also removes linear phase distortions (frequency-dependent phase shifts) across any cross section parallel to the F_2 dimension[11,12,15,16] and hence appears preferable. Applying the Carr–Purcell–Meiboom–Gill modification to the re-

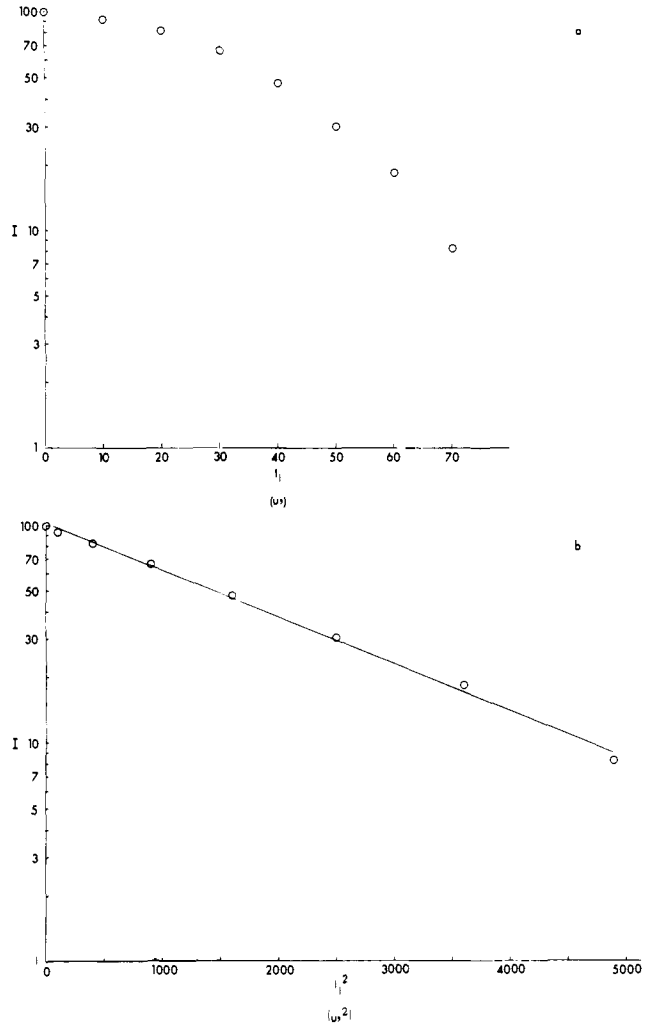

Figure 3. For the C-2,6 ring carbons in 4-ethoxyphenylacetic acid (**5**), plot ln I vs. t_1 (a) and plot of ln I vs. t_1^2 (b).

Table II. Calculated Decay Rate (μs) and Calculated Time (μs) Required for Carbon Atom Signal Intensity in Various Functional Groups To Decay by 50 and 75%[a]

functional group	calcd decay rate	calcd 50% decay	calcd 75% decay
CH_2[b]	12–29	14–33	20–48
	(12–16)	(14–19)	(20–27)
CH[b]	15–32	20–40	26–55
	(15–24)	(20–29)	(26–41)
non-*tert*-butyl CH_3[c]	50–121	40–92	78–172
	(50–121)	(40–88)	(78–172)
	64[17]	not reported[17]	not reported[17]
tert-butyl CH_3	91	63	126
fast component[d]	1462	1013	2026
slow component[d]	231[17]	not reported[17]	not reported[17]
nonprotonated sp^3	46	32	66
fast component[d]	1351	936	1872
slow component[d]	252[17]	not reported[17]	not reported[17]
nonprotonated[e] sp^2	75–218	56–163	108–314
	(75–218)	(56–163)	(108–314)
	83–193[17]	not reported[17]	not reported[17]

[a] Values in parentheses do not include data for **5**, many of whose signals decay relatively slowly. [b] According to eq 2. [c] According to eq 1. [d] According to eq 3. [e] Not reported in ref 17.

(50) Bodenhausen, G.; Freeman, R.; Niedermeyer, R.; Turner, D. L. *J. Magn. Reson.* **1976**, *24*, 291–294.
(51) Müller, L.; Kumar, A.; Ernst, R. R. *J. Magn. Reson.* **1977**, *25*, 383–390.
(52) Turner, D. L.; Freeman, R. *J. Magn. Reson.* **1978**, *29*, 587–590.

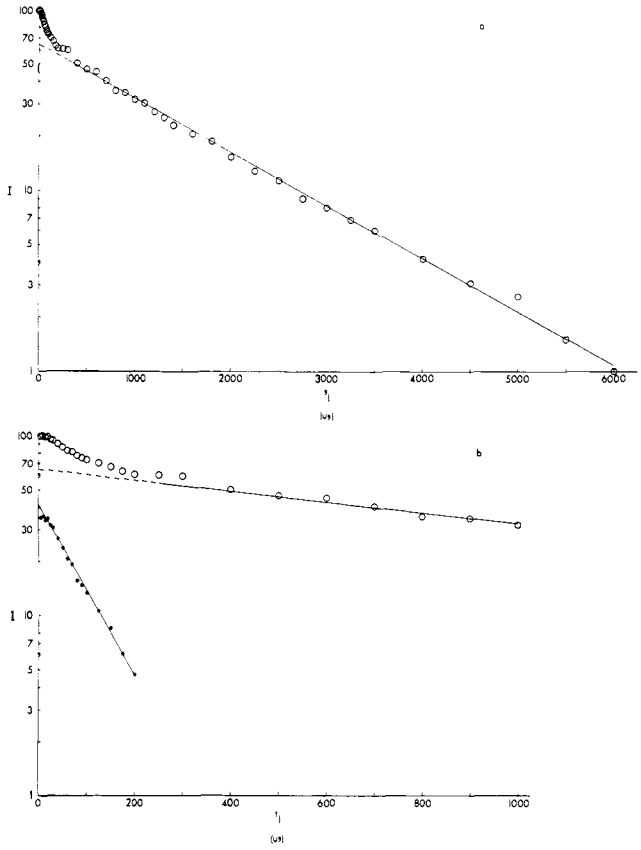

Figure 4. (a) Plot of ln I vs. t_1 for the methyl carbons in bis(3,5-di-*tert*-butyl-4-hydroxybenzyl) ether (**4**). (b) Expanded plot of part of Figure 4a: the circles designate experimental data; the solid line through the circles represents the least-squares fit of the experimental data for the slowly decaying component ($250 \leq t_1 \leq 6000$ μs); the dashed line is the extrapolation of the solid line; the asterisks designate the calculated data for the rapidly decaying component; and the solid line through the asterisks represents the least-squares fit of the calculated data for the rapidly decaying component.

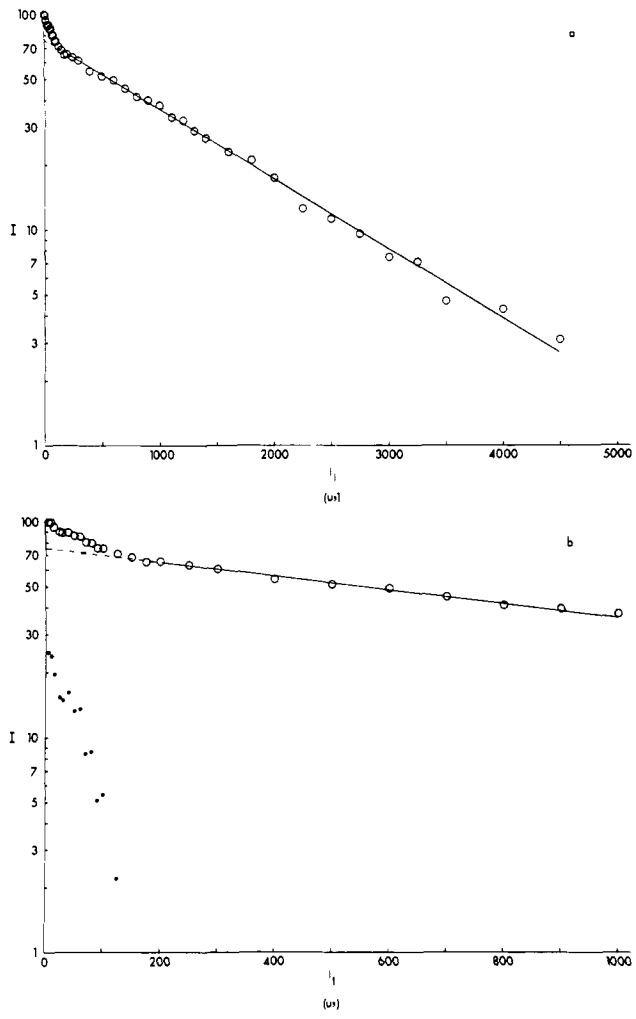

Figure 5. (a) Plot of ln I vs. t_1 for the quaternary aliphatic carbons in bis(3,5-di-*tert*-butyl-4-hydroxybenzyl) ether (**4**). (b) Expanded plot of part of Figure 5a: the circles designate experimental data; the solid line represents the least-squares fit of the experimental data for the slowly decaying component ($200 \leq t_1 \leq 4500$ μs); the dashed line is the extrapolation of the solid line; and the asterisks designate the calculated data for the rapidly decaying component.

focusing pulse gives the proper signal intensity even if the pulse is not exactly 180°.[53] For a solid, this modification consists of turning off both rf fields for a time $t_1/4$, applying refocusing pulses to both spins, turning off both rf fields for a time $t_1/2$, again applying refocusing pulses to both spins, turning off both rf fields for the final time $t_1/4$, and then acquiring the FID for the S spin with heteronuclear decoupling for a time t_2.

The amplitudes of signals in $S(t_1,F_2)$ spectra also can be modulated[54] by magic angle sample spinning used to reduce chemical shift anisotropy.[55] Therefore, a train of rotational echoes at integral multiples of the spinner period occurs in the dipolar t_1 dimension.[11,12,16] Thus, dipolar and rotational echoes are superimposed on the decay of the signal amplitude with increasing t_1 for cross sections parallel to t_1 and through the spectral signal. Consequently, a complex decay pattern[6,11,12,16] consisting of two minima and a minor maximum are sometimes seen before the first rotational echo appears at $t_1 = 1/\omega_r$. These features are present if the dipolar modulation is strong enough between the rotational echo at $t_1 = n/\omega_r$ and the following echo at $t_1 = (n + 1)/\omega_r$.[11,12,16]

In addition to the papers cited on two-dimensional NMR of solids, other related papers have appeared.[56-58]

(53) Farrar, T. C.; Becker, E. D. "Pulse and Fourier Transform NMR: Introduction to Theory and Methods"; Academic Press: New York, 1971; Chapter 2.
(54) Kumar, A.; Ernst, R. R. *Chem. Phys. Lett.* **1976**, *37*, 162-164.
(55) Andrew, E. R.; Bradbury, A.; Eades, R. G. *Nature (London)* **1959**, *183*, 1802-1803.
(56) Waugh, J. S. *Proc. Natl. Acad. Sci. U.S.A.* **1976**, *73*, 1394-1397.
(57) Opella, S. J.; Waugh, J. S. *J. Chem. Phys.* **1977**, *66*, 4919-4924.
(58) Linder, M.; Höhener, A.; Ernst, R. R. *J. Chem. Phys.* **1980**, *73*, 4959-4970.

Experimental Section

The significant compounds discussed in this paper are numbered as shown in Figure 2. Spectra of **1-4** were acquired with the Bruker CXP-100 spectrometer and Z32 PE/MAS probe previously described.[1] Spectra of **5** were acquired with this spectrometer and a probe built in this laboratory. All five compounds were studied with the pulse sequence shown in Figure 1b with a 4K data table (usually a zero-filled 1K or 2K data table), a rf field of 50 kHz for ^{1}H spin locking and decoupling, a contact time[49] of 3 ms, 12-bit digitizer resolution, and a delay time of 3 s between the end of the data acquisition and the 90° proton pulse beginning the next cycle. The spectra of **1** (Figure 8) and **5** (Figure 7) reflect the line broadening factors of 5 and 3 Hz, respectively.

Results and Discussion

Table I contains dipolar dephasing times for five compounds with a variety of simple functional groups. As expected, the various types of carbons experience a wide range of ^{13}C–^{1}H dipolar interactions. In addition, methyl and nonprotonated carbons each exhibit a remarkable range of dipolar dephasing times.

The data for carbons weakly coupled to protons follow a single exponential law before the first rotational echo:

$$I = I_0 e^{-t_1/T_2'} \quad (1)$$

where I_0 is the signal intensity at zero time and T_2' is the exponential decay constant for the signal intensity. When the carbons are strongly coupled to protons, the signal decay frequently is

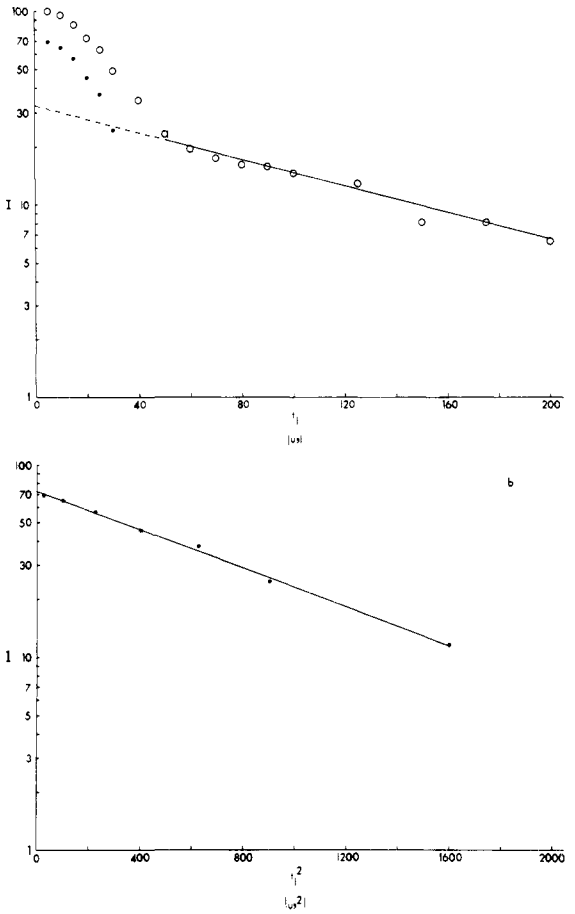

Figure 6. (a) Plot of ln I vs. t_1 for the resonance band arising from the C-1 and C-2,6 ring carbons (circles) and for just the C-2,6 ring carbons (asterisks) in bis(3,5-di-*tert*-butyl-4-hydroxybenzyl) ether (**4**). The solid line represents the least-squares fit of the experimental data for the slowly decaying component (C-1); the dashed line is the extrapolation of the solid line. The anomalous data point at t_1 = 150 μs was not used in the calculation of the least-squares equation. (b) Plot of ln I vs. t_1^2 for the C-2,6 ring carbons in **4**.

modulated by the strong ^{13}C–^{1}H dipolar coupling, and the overall decay of the signal in the short time limit is better described by the equation:

$$I = I_0 e^{-t_1^2/(2T_2^2)} \tag{2}$$

For the *tert*-butyl carbons studied, dipolar modulation is negligible, and the decay curves are biexponential and exhibit two significantly different time constants, T_{2A}' and T_{2B}':

$$I = I_{0A} e^{-t_1/T_{2A}'} + I_{0B} e^{-t_1/T_{2B}'} \tag{3}$$

A. CH and CH_2 Carbons. As reported previously, CH and CH_2 carbon atoms are strongly coupled to protons and therefore dephase more rapidly in the absence of a proton locking field.[1,8,9,11-14,17] Destructive interference arising from the dipolar interactions causes the disappearance of most CH_2 carbon signals after 35 μs, aromatic CH carbon signals after 40 μs, and the aliphatic CH carbon signal after 55 μs. Opella and Frey[8] indicate that other aliphatic CH carbon signals disappear within 40–45 μs. Indeed, as one report[13] noted, the dipolar dephasing experiment is "extremely discriminating when a delay time of ca. 40 μs is used." Exception to this rule may occur if the molecule rapidly reorients in the crystalline state,[3] but generally only molecules with high symmetry can undergo such motion. In the nearly spherical norbornadiene (**6**), the CH_2 carbon signal disappears after about 1000 μs at 200 K when the proton locking field is suspended. The aliphatic CH carbon signal lasts about 1400 μs, and the olefinic CH carbon signal persists for a considerably longer time. Because molecular tumbling attenuates the effective ^{13}C–^{1}H dipolar interaction, all three types of carbon atoms also polarize extraordinarily slowly in conventional cross polarization experiments.

Dipolar dephasing and conventional cross polarization experiments can also provide significant complementary information about motional freedom in molecules tumbling less rapidly than norbornadiene. Both experiments also have shown that an isopropyl CH has a weaker effective dipolar interaction than an aromatic CH.[1] Internal motion of the isopropyl group could account for these weaker effective interactions. In 4-butoxybenzoic acid (**2**), the cross polarization times [$T_{CH}(\alpha\text{-}CH_2) < T_{CH}(\beta\text{-}CH_2) < T_{CH}(\gamma\text{-}CH_2)$] correlate nicely with the dipolar dephasing times [$T_2(\alpha\text{-}CH_2) < T_2(\beta\text{-}CH_2) < T_2(\gamma\text{-}CH_2)$] as one moves along the aliphatic chain. Segmental motion in the chain could account for these results. A recent report[59] indicates in norvaline, $H_3N^+CH(CH_2CH_2CH_3)COO^-$, that $T_1(\gamma\text{-}CH_2) > T_1(\beta\text{-}CH_2)$, in agreement with the 4-butoxybenzoic acid data.

It has previously been noted[17,37] that the signal intensity of CH and CH_2 carbons is better described by eq 2 than by eq 1, and our data confirm this conclusion. A plot of ln I vs. t_1 for the C-2,6 ring carbons of **5** yields a curve (Figure 3a) that exhibits a steadily increasing rate of decay in accordance with eq 2. The least-squares fit of data in the range 0–60 μs has a correlation coefficient of −0.959. In contrast, a plot of ln I vs. t_1^2 from eq 2 yields a curve (Figure 3b) that is highly linear over the range 0–70 μs with a correlation coefficient of −0.999. The value of T_2' from Figure 3a is comparable with T_2 from Figure 3b, and this was found to hold for other strongly coupled carbons.

Dipolar modulation of each carbon-13 spin by the local protons

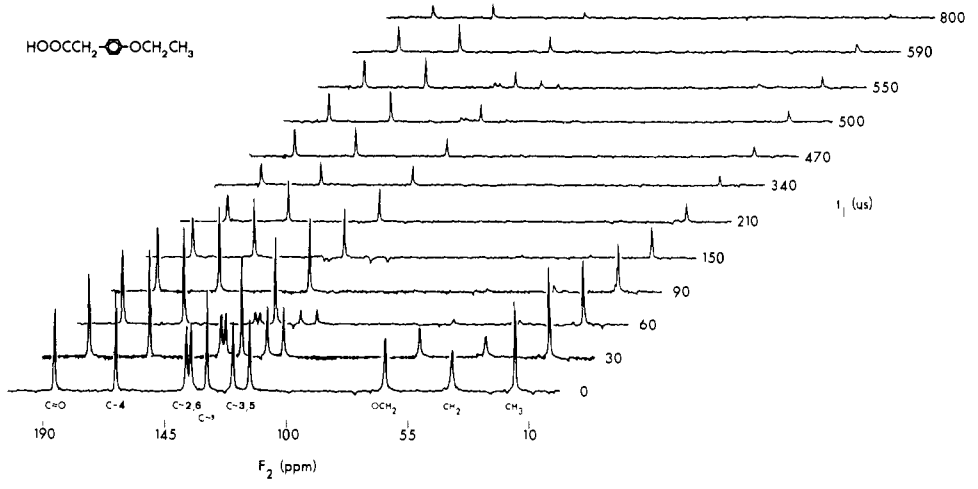

Figure 7. The conventional cross polarization (t_1 = 0) and selected dipolar dephasing spectra of 4-ethoxyphenylacetic acid (**5**). For any cross section parallel to t_1 and through a signal, the dipolar and rotational echoes are superimposed on the decay of the signal amplitude with increasing t_1.

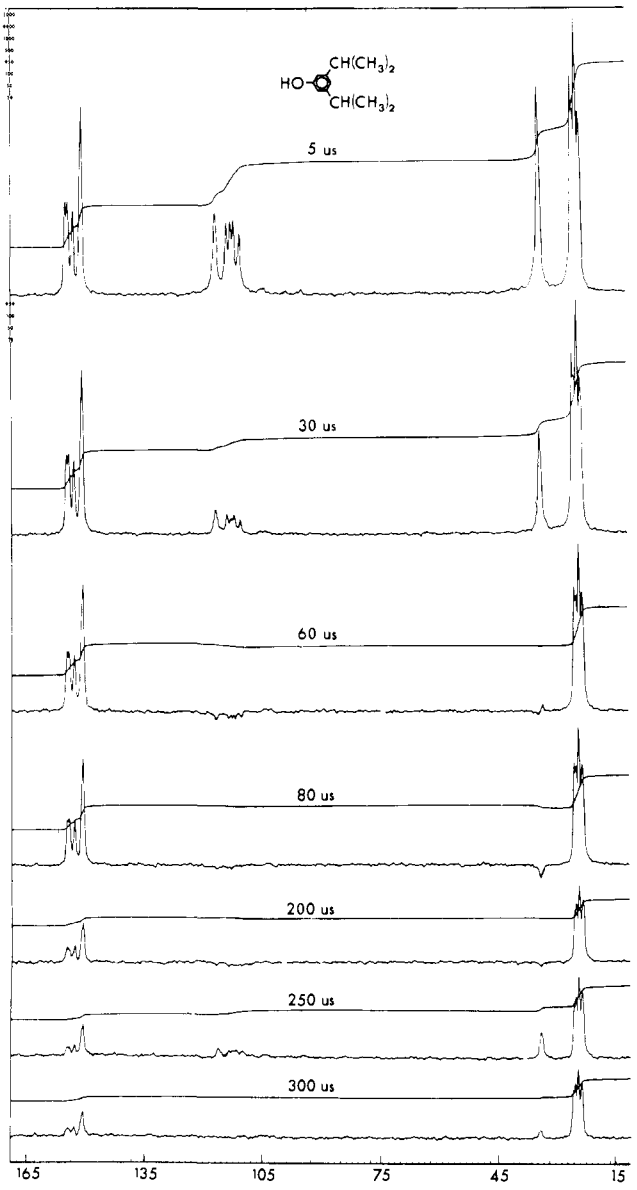

Figure 8. Selected dipolar dephasing spectra of 3,5-diisopropylphenol (**1**). For any resonance, the dipolar and rotational echoes are superimposed on the decay of its intensity with increasing t_1.

can be expected to follow a cos ωt_1 dependence. Summing over all orientations of the crystallites yields the following function for the decaying signal:

$$I = \sum_i I_{0,i} \cos \omega_i t_1 = \sum_i I_{0,i}\left(1 - \frac{\omega_i^2 t_1^2}{2!} + \frac{\omega_i^4 t_1^4}{4!} - + \ldots\right) \simeq I_0 - \sum_i \frac{I_{0,i}\omega_i^2}{2} t_1^2 \quad (4)$$

For very short times, the higher order terms in the expansion vanish, and I shows a quadratic dependence on time. Equation 2 also has the same analytical form for short times. Thus,

$$I = I_0 e^{-t_1^2/(2T_2^2)} = I_0\left(1 - \frac{t_1^2}{2T_2^2} + \frac{t_1^4}{2^2 2! T_2^4} - + \ldots\right) \simeq I_0 - \frac{I_0}{2T_2^2} t_1^2 \quad (5)$$

Thus, in the short time limit, one may relate T_2 with ω_i and the weighting factors, $I_{0,i}$, as follows:

$$\frac{1}{T_2^2} = \sum_i \frac{I_{0,i}\omega_i^2}{I_0} \quad (6)$$

Thus, $1/T_2$ may be considered to be a root mean squared average of ω_i properly weighted by the fraction $(I_{0,i}/I_0)$ of molecules with a given orientation having the dipolar modulation frequency, ω_i. Summing over various orientations yields destructive interference between various crystallites that rapidly attenuates the signal. However, appropriate π pulses on both the carbons and protons at time $t_1/2$ can refocus the local dipolar order in the carbon spins into an echo at t_1. The echo will be attenuated by random $T_{1\rho}$ processes associated with relaxation of the carbon spin in the local proton dipolar fields. The signal intensity for strongly coupled carbons usually decays within 50 μs, and therefore the short time assumption embodied in eq 4 and 5 is reasonable, as higher order terms are negligible.

B. CH_3 Carbons. Previous reports have indicated that methyl carbon atoms usually experience an effective ^{13}C–^1H dipolar coupling that has been attenuated owing to rotational motion. The results obtained with five types of methyl groups in **1**–**5** indicate (Table I) that molecular structure greatly influences these effective dipolar interactions, presumably through changes in the barrier to methyl rotations.

The tolyl methyl carbons in **3** and the methyl carbon terminating the *n*-butoxy chain in **2** apparently experience dipolar interactions of similar magnitude, yielding values for T_2' of 50 and 70 μs, respectively. These methyl values are clearly longer than the decay rates found for any of the CH or CH_2 carbons (Table II).

The methyl carbon terminating the ethoxy chain in **5** seems to experience a somewhat weaker effective dipolar interaction as indicated by a T_2' value of 109 μs. The T_2' value for the isopropyl methyl carbon in **1** is 121 μs, similar to the methyl value in **5**, and therefore, ethyl and isopropyl methyls do not appear to differ greatly. It has already been observed[13] that the signal for the methine carbon in the isopropyl group in 1,4-bis(*N*-isopropylamino)anthraquinone (**7**) decays much faster than the methyl signal.

C. Tertiary Butyl Groups. The methyl carbons in the *tert*-butyl group of **4** clearly experience an even weaker effective dipolar interaction than the methyls discussed above (Tables I and II). The T_{2A}' and T_{2B}' values are 91 and 1462 μs. Conventional cross polarization studies of **4** and di-*tert*-butyl oxalate (**8**) indicated greater motion for *tert*-butyl methyls, as rapid rotation of each methyl group and of the *tert*-butyl group itself about its C_3 axis strongly attenuates the dipolar interaction.[1,2] Indeed, the effective interaction is so weak that, without proton locking, the signal for the methyl carbons and the signal for the quaternary aliphatic carbons of **4** decay at *virtually the same rate.* The data are consistent with the conventional cross polarization studies which indicated that *tert*-butyl methyl carbons polarize only slightly faster than quaternary aliphatic carbons. Not surprisingly, in *p*-di-*tert*-butylbenzene (**9**), the signal for the methyl carbons decays only slightly faster than the signal for the quaternary aliphatic carbons (Table II).[17]

Quantitative assessments of the decay rates for the signal for the methyl carbons and the signal for the quaternary aliphatic carbons in **4** and **9** appear in Tables I and II. Unlike simple methyls, a plot of ln I vs. t_1 for the *tert*-butyl methyl carbons of **4** yields a decay that is clearly biexponential (Figure 4a). Extrapolation of the linear portion of the log plot ($r = -0.998$) for the slowly decaying methyl carbon signal ($250 \leq t_1 \leq 6000$ μs) to $t_1 = 0$ gives $I_0 = 0.65$. This is interpreted as indicating that two methyl groups of each *tert*-butyl group apparently experience a much weaker ^{13}C–^1H dipolar interaction than the remaining third methyl group, suggesting that two methyl groups of each *tert*-butyl group may have more motional freedom. The hydroxyl group ortho to the *tert*-butyl groups most likely requires two methyl carbons of each *tert*-butyl group to be on either side of the plane of the aromatic ring and the remaining methyl carbon to be forced in the plane of the ring close to a ring proton.[60] This structure could cause motional inequivalence among the methyl groups[60]

(59) Ganapathy, S.; McDowell, C. A.; Raghunathan, P. *J. Magn. Reson.* **1982**, *50*, 197–211.

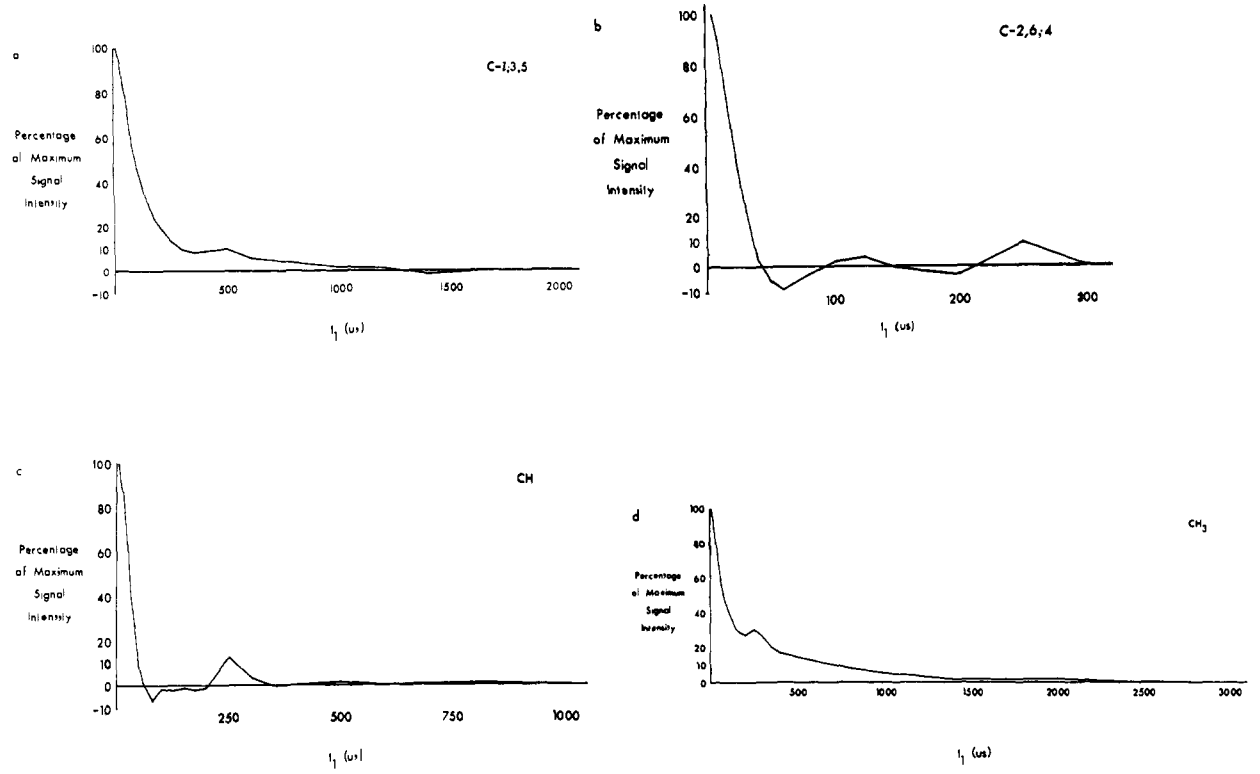

Figure 9. (a) Plot of the nonprotonated aromatic carbon signal intensity in 3,5-diisopropylphenol (**1**) as a function of t_1 (C-1 and C-3,5 overlap). (b) Plot of the protonated aromatic carbon signal intensity in **1** as a function of t_1 (C-2,6 and C-4 overlap). (c) Plot of the aliphatic CH carbon signal intensity in **1** as a function of t_1. (d) Plot of the methyl carbon signal intensity in **1** as a function of t_1.

and alter the relaxation parameter accordingly. A motionally restricted methyl group would generate a stronger ^{13}C–^{1}H dipolar interaction and contribute to a rapidly decaying (shorter T_{2A}') component superimposed on a slower component, as observed in Figure 4a. These data are qualitatively similar to data demonstrating methyl carbon inequivalence in **10**.[60]

The higher symmetry of **9** (equivalent ring protons on either side of a *tert*-butyl group) removes the constraint on the orientation of the *tert*-butyl group and generates just a rotational barrier with simple threefold degeneracy for the *tert*-butyl group. Consequently, a plot of ln I vs. t_1 for **9** should yield a simple exponential decay.

A plot of ln I vs. t_1 for the *tert*-butyl quaternary carbon of **4** also yields a decay that is clearly biexponential (Figure 5a). The six rapidly rotating protons of the *tert*-butyl group have a substantially weaker dipolar interaction with the quaternary carbon than the three relatively slowly rotating protons have. These two types of protons do not contribute in a simple 2:1 ratio to the dipolar interaction, for extrapolation of the linear portion of the log plot ($r = -0.998$) for the slowly decaying quaternary carbon signal ($200 \leq t_1 \leq 4500$ μs) to $t_1 = 0$ gives $I_0 = 0.76$.

D. Nonprotonated sp^2-Hybridized Carbons. Compound **4** provides also an example of overlapping resonances (C-1 and C-2,6) that exhibit a rapidly decaying (C-2,6) and a slowly decaying (C-1) component (Figure 6a). Extrapolation of the linear portion of the plot ($r = -0.994$) for the C-1 carbon ($50 \leq t_1 \leq 200$ μs) to $t_1 = 0$ gives $I_0 = 0.32$ in accordance with the carbon atomic ratio. Subtraction of the extrapolated C-1 signal for t_1 values less than 50 μs gives an estimate of the signal intensity arising only from C-2,6 (Figure 6a), and the decay of this portion of the signal intensity exhibits the quadratic dependence upon time typically exhibited by CH and CH_2 carbons (cf. Figure 3a). A plot of ln I vs. t_1^2 for this portion of the curve (Figure 6b) yields a highly linear plot (cf. Figure 3b) with $r = -0.999$. Treated with an exponential law (eq 1), the data yield $r = -0.967$.

In **1**–**5**, all of the signals for the nonprotonated aromatic carbons decay more rapidly than the signal for the *tert*-butyl methyl carbons in **4** (Table I). Similarly, in **9**, the nonprotonated aromatic carbons have a shorter T_2' (193 μs) than the methyl carbons (T_2' = 231 μs).[17] Nevertheless, for nonprotonated aromatic carbons the structure substantially influences the dipolar-induced relaxation processes. In **4**, the T_2' values are 218 and 211 μs for C-3,5 and C-4, respectively. In contrast, the signal for nonprotonated aromatic carbons near more protons decays much more rapidly. For example, the T_2' value for C-1 in **4**, which is adjacent to CH_2 protons and to two aromatic CH protons, is 126 μs. In the compounds studied, nonprotonated aromatic carbons near several protons exhibit a range of decay rates (T_2' = 75–185 μs). Among the nonprotonated aromatic carbon atoms adjacent to CH_2 or sandwiched between two aromatic CH protons, only those in **5** give signals that decay relatively slowly. In **5**, both C-1 and C-4 are adjacent to two aromatic CH groups, but C-1 is also adjacent to a CH_2 group, causing the signal for C-1 to decay more rapidly (T_2' = 167 μs) than the signal for C-4 (T_2' = 185 μs; see Figure 7). Conventional cross polarization studies show that C-1 polarizes more rapidly than C-4.[1]

Tables I and II also contain data for the nonprotonated carbonyl carbons in **2** and **5**. T_2' for the carbonyl carbon atoms in **2** and red clover seeds[19] is about 150 μs. In contrast, the signal for the carbonyl carbon atom in **11** apparently decays more rapidly (T_2' = 83 μs),[17] while the signal for the carbonyl carbon atom in **5** decays considerably more slowly (T_2' = 169 μs). The most slowly decaying carbonyl signal among **2**, **5**, and **11** is for a carbonyl carbon adjacent to a CH_2 group, indicating the need for caution in comparing dipolar dephasing data from different molecules. The very slow dipolar dephasing rates for many of the carbons in **5** (Tables I and II) suggest an unusually high degree of motional freedom for this compound.

E. Dipolar and Rotational Modulation. As noted earlier, dipolar and rotational echoes are superimposed on the decay of the signal amplitude with increasing t_1. Excellent illustrations of such echoes in spinning powders[11,12,16] and a static single crystal[6] have previously appeared, and Figures 7 and 8 illustrate these features for **1** and **5**.

Figure 7 shows for **5**, as expected, that the nonprotonated carbon

(60) Beckmann, P.; Ratcliffe, C. I.; Dunell, B. A. *J. Magn. Reson.* **1978**, *32*, 391–402.

signals (C=O, C-4, and C-1) decay very slowly; the methyl carbon signal decays more rapidly; and the aromatic CH and methylene carbon signals decay the fastest. The dipolar modulation is particularly evident in **5** for the protonated aromatic resonances C-2,6 and C-3,5. The rotational modulation at $2/\omega_r$ (about 560 μs) is also evident. The same phenomena are evident in Figure 8 for **1**. The rotational modulation at $1/\omega_r$ (about 250 μs) is clearly evident. Previous work[6,11,12,16] and Figures 7 and 8 show that a high S/N ratio is usually required to detect the modulation effects. Plots of the signal intensities in **1** as a function of t_1 appear for the nonprotonated ring carbons in Figure 9a, for the protonated ring carbons in Figure 9b, for the methine carbons in Figure 9c, and for the methyl carbons in Figure 9d. For each of the four resolved carbon signals, the decay of the signal amplitude is clearly modulated. The rotational modulation at $2/\omega_r$ is clearly evident in Figures 9a and 9c. The dipolar modulation involving both positive and negative signals is evident in Figures 9a-c. As expected, the CH carbons exhibit the strongest dipolar modulation. The data shown in Figure 8 and the decay patterns shown in Figures 9a-c adequately demonstrate the well-documented dipolar modulation effects[6,11,12,16] and provide approximate dipolar coupling constants. The decay patterns in Figures 9a-d represent cross sections parallel to the t_1 axis of constant F_2, and therefore constitute a free induction decay in t_2. Fourier transformation of these data gives a dipolar spectrum.[6,11,12,16] Finally, we note that the data in Tables I and II are not relevant to experiments in which spin diffusion among the protons during t_1 is suppressed.[16]

Conclusions

Both conventional cross polarization and dipolar dephasing studies at a variety of contact or delay times, respectively, provide information on the magnitude of the $^{13}C-^{1}H$ dipole-dipole interactions. Such information greatly facilitates signal assignments[1,8-10,14,25,26] and provides valuable insights into the proton environment and into the extent of motional freedom in the solid. The application of these techniques to complex solids that cannot be adequately characterized by other methods has been and should continue to be very useful. For example, these results and others[8,9,11-14,17] strongly suggest that spectra obtained under conventional conditions and under a 55-μs suspension of the proton locking field will reveal, respectively, all the carbon atoms and the somewhat attenuated signals of only methyl and nonprotonated carbon atoms. Slightly shorter dephasing periods also suffice in some instances, depending upon the degree of motional freedom present in the sample.

Acknowledgment. We are pleased to acknowledge very helpful discussions with Drs. Kurt W. Zilm and Michael A. Wilson. Support for this work was provided by the Office of Energy Research, U. S. Department of Energy, under Contract No. DE-AS02-78ER05006.

Registry No. 1, 26886-05-5; **2**, 1498-96-0; **3**, 538-39-6; **4**, 6922-60-7; **5**, 4919-33-9; **6**, 121-46-0; **7**, 14233-37-5; **8**, 691-64-5; **9**, 1012-72-2; **10**, 128-37-0; **11**, 626-51-7.

Acetylene and Ethylene Complexes of Gold Atoms: Matrix Isolation ESR Study

Paul H. Kasai

Contribution from IBM Instruments, Inc., Danbury, Connecticut 06810. *Received April 15, 1983*

Abstract: Gold atoms were trapped in argon matrices containing ethylene or acetylene and were examined by electron spin resonance spectroscopy. The spectral analyses revealed formations of π-coordinated gold(0)-mono(ethylene), gold(0)-mono(acetylene), and gold(0)-bis(ethylene) complexes and, in matrices of high acetylene concentration, gold(0)-acetylene adduct of the vinyl form. The **g** tensors and the Au-197 hyperfine coupling tensors of these compounds were determined and analyzed. The monoligand complexes, $Au(C_2H_4)$ and $Au(C_2H_2)$, are held primarily by the dative interaction between the filled d_{xy} orbital of the metal and the antibonding π_y^* orbital of the ligand. The semifilled orbital is an sp-hybridized orbital of the metal pointing away from the ligand. In bis(ethylene)gold(0) the metal atom is flanked by two ligand molecules oriented parallel to each other. The complex is held by the dative interaction between the semifilled p_x orbital of the metal parallel to the ligands and the antibonding π_y^* orbitals of the ligands.

Metal atom chemistry in which vaporized metal atoms are trapped and allowed to react with molecules condensed at cryogenic temperature has been the subject of many recent reports.[1-5] Elucidation of the structure and the orbital property of complexes between transition-metal atoms and unsaturated organic molecules is of particular interest because of its relevance to organometallic syntheses and transition-metal catalysis. IR and UV-visible spectra of ethylene complexes of Cu, Ag, and Au atoms and acetylene complexes of Ni and Cu atoms have been analyzed by Ozin and his co-workers.[6-8]

Electron spin resonance (ESR) spectra of acetylene and ethylene complexes of Cu and Ag atoms generated in rare gas matrices have also been reported.[9] The ESR study showed that Cu atoms form both mono- and diligand complexes with either acetylene or ethylene. Structural features of these complexes have been elucidated as follows.

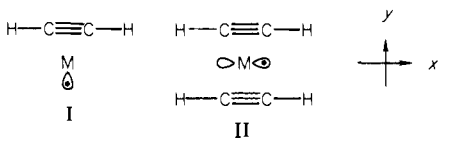

In structure I the unpaired electron is located in an sp_y orbital of the metal atom pointing away from the ligand, and in structure

(1) *Angew. Chem., Int. Ed. Engl.*, **1975**, *14*, 273, a collection of review articles on the subject.
(2) Moskovitz, M.; Ozin, G. A. "Cryochemistry"; Wiley: New York, 1976.
(3) Ozin, G. A. *Acc. Chem. Res.* **1977**, 10, 21.
(4) Moskovitz, M. *Acc. Chem. Res.* **1979**, *12*, 229.
(5) Klabunde, K. J. "Chemistry of Free Atoms and Particles; Academic Press: New York, 1980.
(6) Ozin, G. A.; Huber, H.; McIntosh, D. *Inorg. Chem.* **1977**, *16*, 3070.
(7) McIntosh, D.; Ozin, G. A. *J. Organomet. Chem.* **1976**, *121*, 127.
(8) Ozin, G. A.; McIntosh, D. F.; Power, W. J.; Messmer, R. P. *Inorg Chem.* **1981**, *20*, 1782.
(9) Kasai, P. H.; McLeod, D., Jr.; Watanabe, T. *J. Am. Chem Soc.* **1980**, *102*, 179.

0002-7863/83/1505-6704$01.50/0